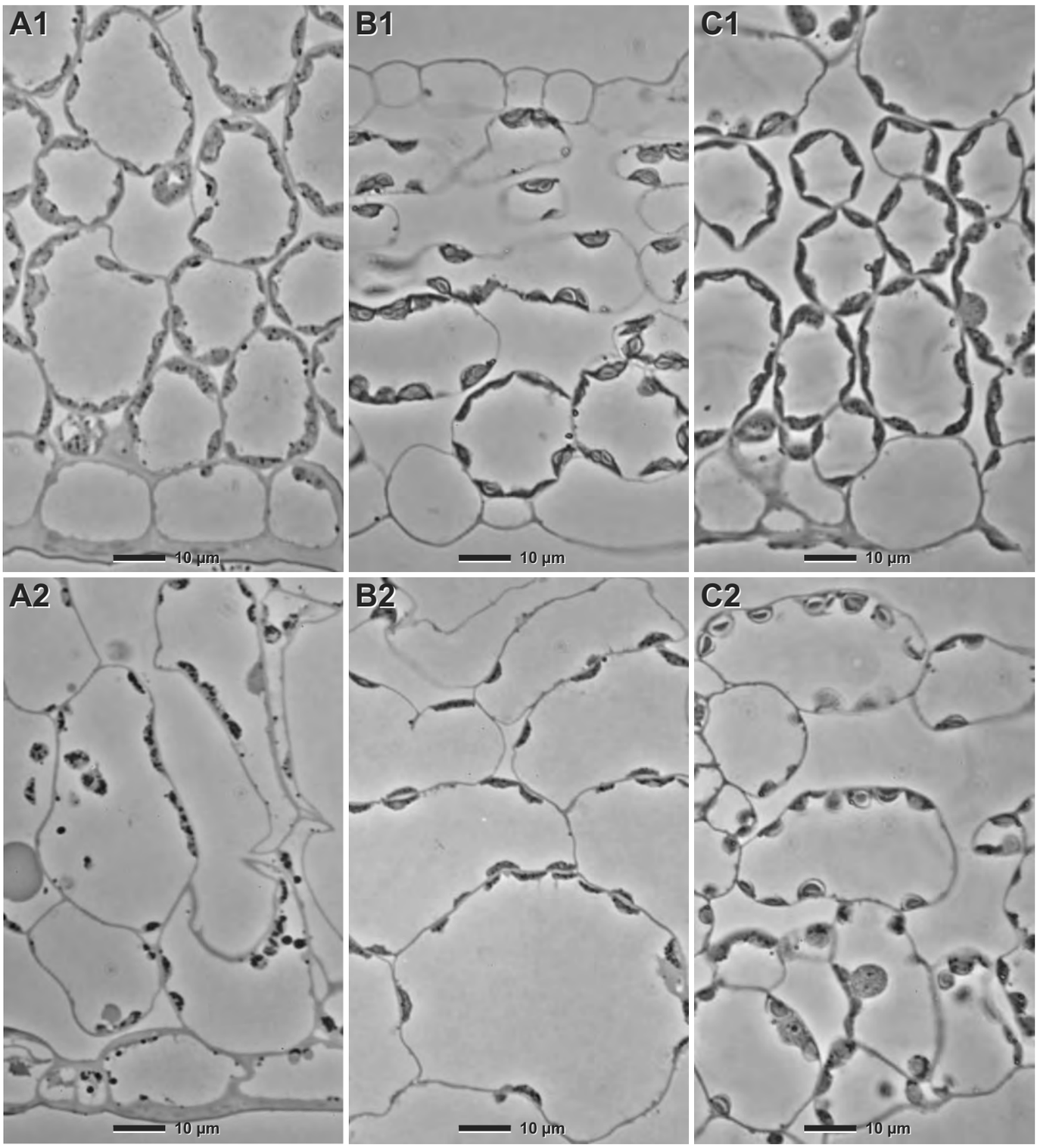

Supplemental Figure 1 online. Representative examples of phase contrast light micrographs of semi-thin cross-sections of leaf sectors of sugar beet (A), *Arabidopsis thaliana* (B) and tobacco (C). Mesophyll of mature (1) and senescent (2) leaves is shown. The lower epidermis is visible at the bottom of A1, B1, C1 and A2, the upper epidermis also on top of B1. Note the enlargement of cells in senescent tissue which in part may result from endopolyploidization (see Supplemental Results online).

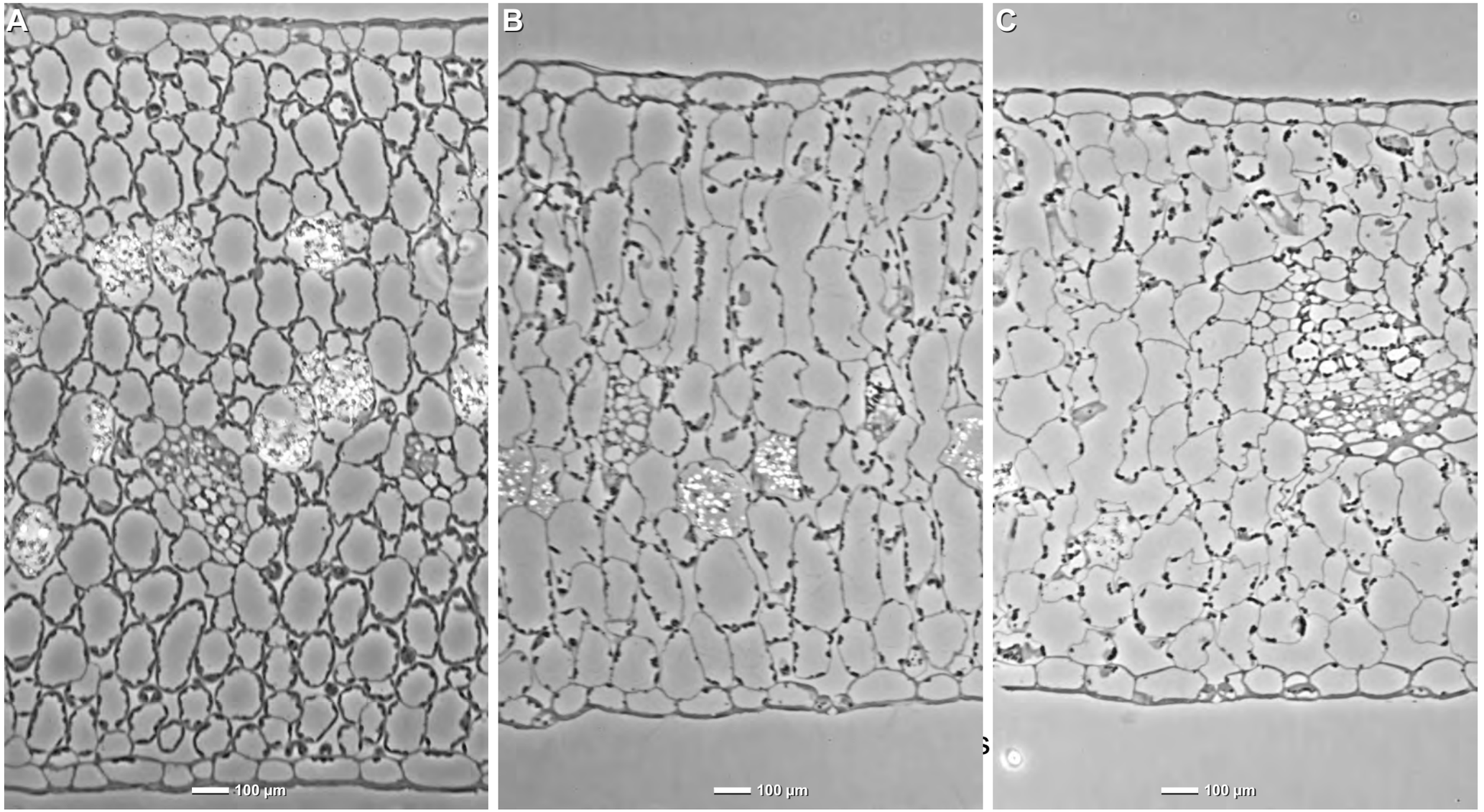

Supplemental Figure 2 online. Representative examples of phase contrast micrographs of semi-thin cross sections of sugar beet leaves: (A) mature leaf (developmental stage III), leaves (B) at an intermediate stage (stage V) and (C) at an advanced stage of senescence (stage V/VI). The different cell sizes reflect probably differences in nuclear ploidy (di- and tetraploidy, respectively).

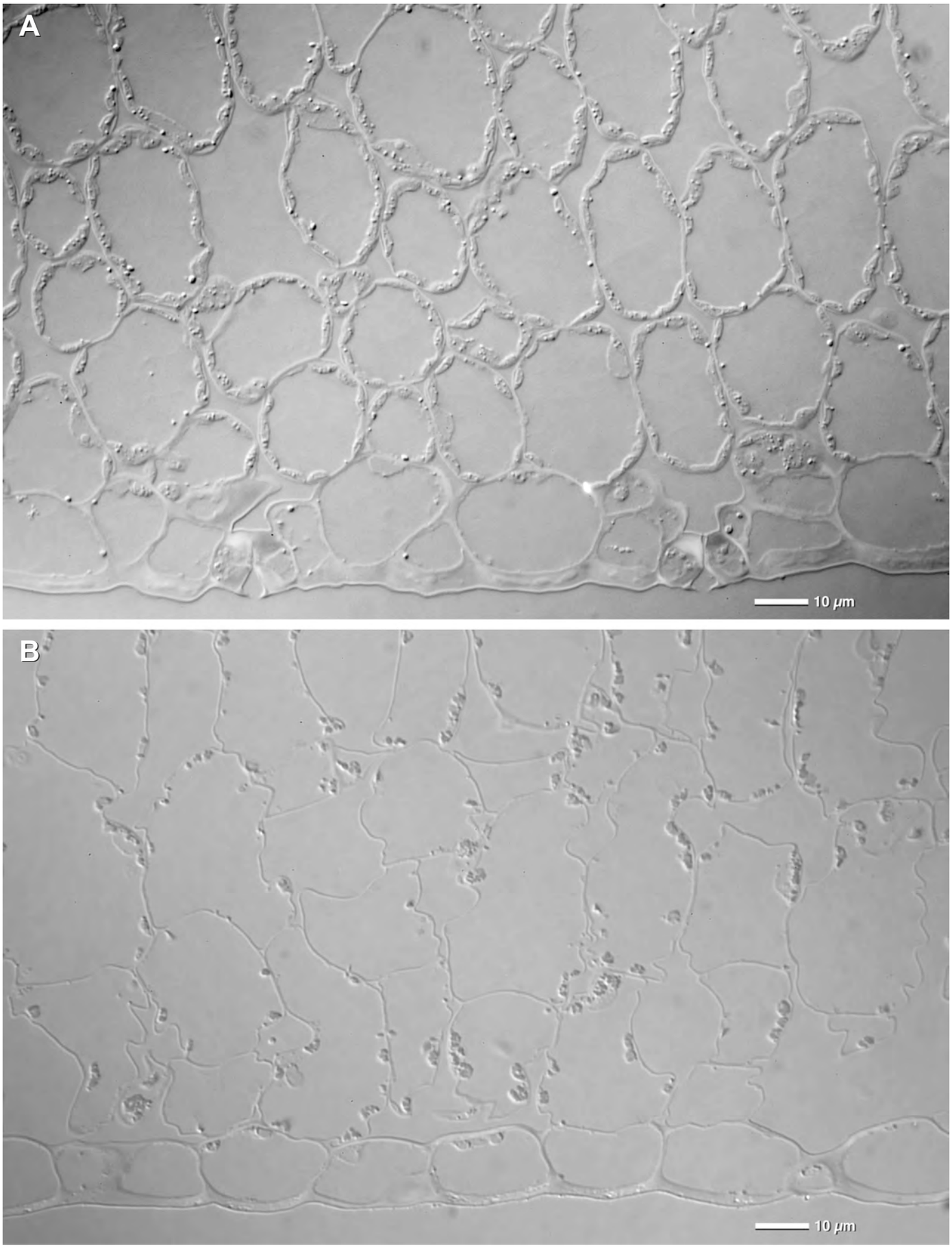

Supplemental Figure 3 online. Representative examples of Noumarski interference contrast micrographs of leaf sectors of sugar beet (A) from a mature leaf (stage IV) and (B) from a highly senescent leaf (stage VI).

SUPPLEMENTAL TABLE 1 ONLINE - Oligonucleotides used for real-time qPCR

name	genome	gene	Sequence (5‘ - 3‘)
Beta vularis			
Bv-clp_fw	plastid	*clpP*	GGC GCC AAG CGT GAG GGA AT
Bv-clp_rev	plastid	*clpP*	TGG GGT TGG CTG CTT CAA TGG G
Bv-ndh_fw	plastid	*ndhH*	CGC CAT AAA AGG GCC GAG CCA
Bv-ndh_rev	plastid	*ndhH*	ACG GAC CGG AAC GTT GGG AA
Bv-psbA_fw	plastid	*psbA*	ACC TAC TAC AGG CCA AGC CGC
Bv-psbA_rev	plastid	*psbA*	AGC CGC TCA TGG TTA TTT TGG TCG
Bv-phyA_fw	nuclear	*phyA*	TCG GCT GCT TGC TTG CCC TC
Bv-phyA_rev	nuclear	*phyA*	TCG CCT ACA CTG GGG ACA GCA T
Nicotiana tabacum			
Nt-clp_fw	plastid	*clpP*	GGC GCC AAG CGT GAG GGA AT
Nt-clp_rev	plastid	*clpP*	TGC ATG GGA TTA GCC GCT TCA ATG G
Nt-ndh_fw	plastid	*ndhH*	AGG GTA GAT CGG CAG CCA CTC C
Nt-ndh_rev	plastid	*ndhH*	ACC TCT TCG AAG CTG CCA CCG
Nt-psbA_fw	plastid	*psbA*	AGC TCC CAC TCA CGA CCC ATG T
Nt-psbA_rev	plastid	*psbA*	GGG AAG CGG CAT CCG TTG ATG A
Nt-rpoT2-syl	nuclear	*RpoT2-syl*	GCC TCA CAC GCC TAC CAG GTG
Nt-rpoT2-syl	nuclear	*RpoT2-syl*	TGT TCC ATT TTG GCA CTC CAA CCC T
Zea mays			
Zm-clp_fw	plastid	*clpP*	GGA CGC GGC TAT TCC GAG GC
Zm-clp_rev	plastid	*clpP*	TTC CCT TGG CGG TTG GCT AAT CTC A
Zm-ndh_fw	plastid	*ndhH*	TCC ATA AGG GAG ATC GGC AGC GA
Zm-ndh_rev	plastid	*ndhH*	AGC TGT CAC AGG TAT GCG AAT GAT GC
Zm-psbA_fw	plastid	*psbA*	AGC ACT GAA TAG GGA ACC GCC GA
Zm-psbA_rev	plastid	*psbA*	TGT ATT CCA GGC AGA GCA CAA CAT CC
Zm-rpoT1_fw	nuclear	*rpoT1*	CCA TCG CGG CCC TAC GTT CC
Zm-rpoT1_rev	nuclear	*rpoT1*	GTT TCT ATG CGG CCG CCG GT

SUPPLEMENTAL METHODS

Supplemental Datasets 1-4 online illustrate the enormous structural and quantitative complexity and variability of plastids and their genome, the plastome, during leaf development. This includes the regulation of the cellular subgenome homoeostasis, i.e. varying ratios of plastid and nuclear genomes, which is an important, but frequently neglected aspect of the partite eukaryotic genomes.

The figures document a developmental series of DAPI-stained leaf mesophyll cells, focusing on the morphologically particularly diverse early and late ontogenetic stages. Their arrangement follows the designation of leaves used in the printed paper: stages y1 - y4 for leaflets early in development, and I - VI for maturing (I), nearly mature (II), adult (III), ageing (IV), senescent (V) and late senescent/necrotic (VI) leaves. Representative examples of leaves for these developmental stages are shown in Figure 1. The datasets for the four plant species studied are presented in groups: Supplemental Dataset 1 online *Beta vulgaris* (sugar beet), Supplemental Dataset 2 online *Arabidopsis thaliana*, Supplemental Dataset 3 online *Nicotiana tabacum* (tobacco) and Supplemental Dataset 4 online *Zea mays* (maize). The samples were taken from fixed leaf tissue, which was enzymatically weakly softened and subsequently flattened by squashing. Squash preparations, which were best to prepare from with *Arabidopsis* and somewhat harder from sugar beet, proved to be advantageous for exposing DAPI-stained DNA regions in plastids. However, squashing may change sizes of cells and organelles to some extent. In general, leaf mesophyll cells are shown, but in a few instances, palisade parenchyma cells were included, documenting that the findings are valid for this cell type as well and thus can be generalized. To facilitate comparisons, all prints are presented with the same magnification (Bars: 5 µm). Four aspects of general interest deserve mention:

(i) Differences in fluorescence emission intensity between individual nucleoids of organelles imply that DNA regions do not represent units of equal ploidy and suggest that higher emission intensities reflect DNA synthesis without nucleoid division and *vice versa*. It should be emphasized, however, that the data cannot distinguish between differences due to transitions between cell cycle stages or distinct developmental situations.

(ii) With cell elongation and after reaching maximal cellular ptDNA content chloroplasts may enlarge without significant increase in DNA content, since the distances between individual DNA regions frequently become larger, but their fluorescence intensity and number remain comparable. However, in older and larger chloroplasts nucleoids may divide further after cessation of organelle division and reach numbers in the order of 40 or more per organelle, apparently also without significant preceding DNA synthesis, as evident by less bright fluorescence emission (Figure 2C and J, Supplemental Datasets 1, 2 and 4 online, panels 42, 47, 52-55, 63, 98, 100, 129).

(iii) The panels also illustrate nuclear endopolyploidization which is an important feature of leaf development (Butterfass, 1979). This process is usually accompanied by an increase in cell size as well as in chloroplast numbers, the latter by a factor of about two, provided that organelle sizes remain more or less constant. In spite of considerable size variation, based on 235 individual mesophyll cells bimodal distributions of both cell sizes and cellular chloroplast numbers (about 30 vs. >50) were noted in sugar beet (e.g., Supplemental Dataset 1 online, panels 27-32 vs. 51-58). They appeared relatively early (at leaf stage y3). In general, chloroplast numbers per cell are a reliable proxy of nuclear ploidy levels (Butterfass, 1979). Tetraploidization increased significantly and may become predominant later (at leaf stage III). On the other hand, a high, more or less continuous heterogeneity of cell sizes and chloroplast numbers was found for *Arabidopsis* (Supplemental Dataset 2 online, panels 91-105; cf. also Pyke and Leech, 1991). It remains to be shown whether and how this unusual and intriguing behavior is correlated with corresponding changes in the degree of ploidy. In this context, it is important to note that that the extensive endopolyploidization observed in *Arabidopsis* (Zoschke et al., 2007) is rather untypical and does not occur in most other plants. Nucleoid numbers of *Arabidopsis* (and tobacco) plastids were generally high (Supplemental Dataset 2 online, panels 84-101; Supplemental Dataset 3 online, panels 111-114, 117, 118). However,

in near-necrotic leaf tissue, gerontoplasts became much smaller and nucleoid numbers as well as DNA amounts per organelle declined substantially, consistent with a correlation between organelle size and ptDNA amount (Supplemental Dataset 2, panels 106-111; cf. also Evans et al., 2010).
(iv) With cell enlargement and leaf aging, cells, although fixed, became more fragile, but cell fragments usually displayed distinct nucleoid patterns in organelles. In near-necrotic leaf sectors, the detectability of DNA spots declined and often a general increase in background fluorescence could be noted (e.g., Supplemental Dataset 1 online, panels 65-83). This is commensurate with qPCR data uncovering that substantial amounts of ptDNA are present in such tissues.

SUPPLEMENTAL REFERENCES

Butterfass, T. (1979). Patterns of chloroplast reproduction. A developmetal approach to protoplasmic plant anatomy. In Cell Biology Monographs. Continuation of Protoplasmatologie, Vol. 6. L.V. Heilbrunn, W. Beermann, and G. Rudkin, eds (Wien, New York, Springer), pp. 205.
Evans, I.M., Rus, A.M., Belanger, E.M., Kimoto, M., and Brusslan, J.A. (2010). Dismantling of *Arabidopsis thaliana* mesophyll cell chloroplasts during natural leaf senescence. Plant Biol. **12:** 1-12.
Pyke, K.A., and Leech, R.M. (1991). Rapid image analysis screening procedure for identifying chloroplast number mutants in mesophyll cells of *Arabidopsis thaliana* (L.) Heynh. Plant Physiol. **96:** 1193-1195.
Zoschke, R., Liere, K., and Börner, T. (2007). From seedling to mature plant: *Arabidopsis* plastidial genome copy number, RNA accumulation and transcription are differentially regulated during leaf development. Plant J. **50:** 710-722.